A COMPUTER MODEL TO PREDICT THE DROPLET SIZE TRAVELING DISTANCE IN NOWIND AND WINDY CONDITIONS FOR DIFFERENT NOZZLE SHAPES.

A. M. El-Berry[1], M. H. Ramadan[2], M. A. El-Adl[3] and H. M. Abdel Mageed[4]

ABSTRACT

A finite difference numerical model was developed to determine the mean droplet size diameter at any distance from a sprinkler as a function of nozzle shape, size and pressure. Droplet size data from square, rectangle, triangle and circle nozzle orifice shapes verified the model. Data for model prediction were generated throughout lab experiments. Nozzle pressure and shape had a major influence on droplet size. Higher pressure promoted smaller droplets over the entire application profile. Noncircular nozzles had a large droplet size at the same distance from sprinkler but circular nozzle had the largest droplet size near the perimeter.

Key words: *sprinkler irrigation, nozzle shape, droplet size, modeling.*

INTRODUCTION

Kohl (1974) studied the effects of pressure and nozzle size on the droplet size distribution from medium sized agricultural sprinklers. He reported that the droplet size distribution from agricultural sprinklers followed the relationship of decreasing droplet size with increasing relative velocity of the water to the air. Decreasing nozzle diameter decreased mean droplet size but increasing pressure decreases mean droplet size by a great amount.

Awady (1978) set two hypotheses for droplet separation: against surface tension and against viscous shear. For surface tension, the droplet size "*S*" varies as:

1 Prof. of Agric. Eng., Dept. of Agric. Eng. , Faculty of Agriculture, Cairo University, 2 and 3 Assoc. Prof. of Agric. Eng. Dept. of Agric. Eng., Faculty of Agriculture, Al-Mansoura University, and 4 Agric. Res. Ins., Alexandria Branch, Alexandria, Egypt

$$S \cong \frac{\delta}{P \tan^2(\alpha/2)} \qquad (1)$$

and for shear :

$$S \cong \frac{\mu}{\sqrt{\rho P} \ \tan(\alpha/2)} \qquad (2)$$

Where "δ" is surface tension, "P" pressure, "α" spray cone angle, "μ" coefficient of dynamic viscosity, "ρ" is the fluid density. Dimensions have to be homogeneous on both sides of the relations.

The critical state beyond 0.25 tend to separation under tension, for the following criterion (C_r):

$$C_r = \frac{\mu}{\delta} \sqrt{\frac{P}{\rho}} \ \tan(\alpha/2) \ \cong \ 0.25 \qquad (3)$$

David and Yuping (1989) reported that nozzle pressure had major influence on droplet size. The volume mean droplet diameter of total water applied as a function of nozzle size and pressure were determined. Higher pressure promoted smaller droplets over the application profile.

Kohl (1974) stated that the droplet mass was important specially on soils with crusting problems; it was very sensitive to water pressure. He also found that the mean size of water droplets is increasing along the trajectory distance. He also found that decreasing nozzle diameter decreased mean droplet size, while increasing pressure decreases mean droplet size by a greater amount, especially at the end of the jet. He found that droplet mass was increased fivefold with a pressure decrease from 60 to 20 N/Cm^2 (MPa). He referred that to the relationship of decreasing droplet size with increasing relative velocity of water to the air.

Droplet size is an important factor affecting the formation of "seals" on bare soil surfaces that restrict water movement into the soil. Because, small droplets possess less power when they impact the soil surface, "seals" that limit infiltration form more slowly than with larger droplets. For these reasons, it is sometimes possible to reduce runoff and erosion by converting from sprinklers that emit large droplets to ones with

186

smaller droplets. Droplet size is especially important when sprinklers must operate in wind. Distribution patterns from sprinklers that emit smaller droplets are more subject to wind distortion and lower application uniformity. In addition, increased losses due to wind drift usually occur with small droplet sprinklers (*Larry, 1988*).

The soil damage hazard from large droplets is further compounded in the case of circular nozzles at low pressures due to high application rates near the perimeter (*Chen and Wallender, 1985*).

Heernann and Kohl (1981). stated that the droplet size distribution of sprinkler is practically important for two reasons:

I- Small droplets are subjected to wind drift, distorting the application pattern.

2- Large droplets possess greater kinetic energy which is transferred to the soil surface causing particle dislodgement and puddling that may result in surface crusting and runoff.

Higher operating pressures normally increase the volume of water applied as smaller droplets while decreasing the volume of larger droplets. A similar, but a significantly smaller effect occurs on the larger droplets (not on the volume of water) as nozzle opening size is decreased. Nozzle opening shape can have an important effect on droplet size while nozzle angle has little effect. (*Larry,1988*)

Diffuse-jet nozzles; are designed so that droplets are formed at a lower pressure than with other impact nozzles. This is accomplished by using noncircular-shaped nozzle openings or turbulence inducer at the orifice to diffuse the jet as it leaves the nozzle. Diffuse-jet nozzles do not wet as large an area as do constant-diameter and constant-discharge nozzles. (*Larry, 1988*)

Low pressure impact sprinklers produce smaller droplets at a lower pressure than do traditional impact sprinklers which operate at 350 kPa (50 psi) or more. This is accomplished by passing water through one or more noncircular shaped nozzles to diffuse the jet as it leaves the sprinkler. These sprinklers operate at about 240 kPa (35 psi) and normally have a wetted diameter of 20 to 25 m (70 to 80 ft) (*James and Blair, 1984*).

Jiusheng, (1997) found that for both circular and square nozzles, increasing pressure decreased droplet size in overall droplet spectra, and for a given pressure, changing nozzle shape from circular to square also decreased droplet size.

Frost and Schwalen (1960) investigated combined spray evaporation and drift losses, also by the catch-can method. A good correlation between spray losses and vapor- pressure deficit was obtained, and it was found that losses were approximately proportional to nozzle pressure and wind speed and inversely proportional to nozzle diameter. ***Seginer (1971)*** reported that as the number of droplets in the air increased and their size decreased, the total loss increased. The regression lines of total loss on solar radiation, for various operation conditions were practically parallel to each other with slope of about 0.5.

Jiusheng Li and Hiroshi Kawano (1995) studied the water droplet movement in the air which is mainly affected by drag and gravity. They used the following equations of motion for an individual droplet under no-wind condition on a computer model.

$$\frac{d^2x}{dt^2} = -3/4 \, (\rho_a/\rho_w) \, . \, (C_d/d) \, . \, V \, . \, V_x \tag{4}$$

$$\frac{d^2z}{dt^2} = -3/4 \, (\rho_a/\rho_w) \, . \, (C_d/d) \, . \, V \, . \, V_z - g \tag{5}$$

Where:

x = position component in the horizontal direction in m,

z = position component in the vertical direction in m,

t = time in s,

$V_x = dx/dt$ = horizontal component of velocity V in m/s, *and*

$V_z = dz/dt$ = vertical component of velocity V in m/s.

Equations (4) and (5) were solved by using Runge-Kutta fourth-order numerical scheme with the time step increment (Δt) of 0.005 s. Finally they predicted the droplet diameter at any distance from sprinkler for circular, square and double rectangular nozzle shapes.

They used the following initial conditions to solve equation (4) and (5) x(0) = 0; z(0) = riser height (0.83 m); $V_X(0) = V(0) \cos \theta_0$; $V_Z(0) = V \sin\theta_0$; θ_0 = sprinkler trajectory angle; V(0) = initial nozzle water velocity (m/s).

188

A finite difference numerical model was developed by ***David and Yuping (1989)*** to determine the volume mean droplet diameter at any distance from a sprinkler as a function of nozzle size and pressure. The model was verified with sprinkler nozzle sizes 4.0 mm and 3.2 mm circular and 3.5 mm square nozzles. A total of 140 indoor tests were conducted with pressure between 69 kPa (10 Psi) and 414 kPa (60 Psi) at 28 kPa (4Psi) increment.

Richards and Weatherhead (1993) studied the effect of wind and reported that wind elongated the pattern at right angles to the wind. The wetted distance downwind from the sprinkler increased as wind velocity increased but the increase was proportionately less than the increase in across wind wetted radius and wetted distance upwind.

The objective of this work is to develop, test, evaluate and verify a computer model to predict the droplet size diameter distribution.

MATERIALS AND METHODS

THE MATHEMATICAL MODEL DEVELOPMENT:
Seginer (1965) obtained a relationship between the empirical drag coefficient " C_n " and droplet diameter as follows:

$$C_n = 0.4671 \, d^{-0.9859} \qquad (6)$$

Where:

$\qquad$ d = droplet diameter in mm

Hills and Yuping (1989) used the following equations relating acceleration of water droplet in the horizontal and vertical directions respectively:

$$A_X = -C_n \, V^2 \cos \theta \qquad (7)$$
$$A_y = -C_n \, V^2 \sin \theta - g \qquad (8)$$

Where:

$\qquad A_x$ = acceleration component in x direction, m/s^2.

$\qquad A_y$ = acceleration component in y direction, m/s^2.

$\qquad$ V = resultant velocity of droplet, m/s. ($V = \sqrt{V_x^2 + V_y^2}$)

$\qquad \theta$ = flight path inclination angle from horizontal ($\theta = \tan^{-1} V_y/V_x$).

$\qquad$ g = gravity acceleration, 9.81 m/s^2.

$\qquad V_x$ = velocity component in x direction, m/s. ($V_x = V \cos \theta$).

$\qquad V_y$ = velocity component in y direction, m/s. ($V_y = V \sin \theta$).

Equations 7 and 8 are rearranged and solved using a numerical finite difference approximation procedure with appropriate initial conditions. For a velocity at time step i; these equations become:

$$V_x (i) = V_x (i-1) + A_X (i-1) \, \Delta t \qquad\qquad (9)$$
$$V_y (i) = V_y (i-1) + A_y (i-1) \, \Delta t \qquad\qquad (10)$$

Where:

$V_X (i-1)$ = velocity component in x direction at time step (i-1), m/s.
$V_y (i-1)$ = velocity component in z direction at time step (i-1), m/s.
$A_X (i-1)$ = velocity component in x direction at time step (i-1), m/s^2.
$A_y (i-1)$ = velocity component in z direction at time step (i-1), m/s^2.
Δt = time step increment, s.

Similarly, the droplet position at time step i is defined by the following equations:

$$X (i) = X (i-1) + X (i-1) \, \Delta t \qquad\qquad (11)$$
$$Y (i) = Y (i-1) + Y (i-1) \, \Delta t \qquad\qquad (12)$$

Where:

$X (i-1)$ = position component in x direction at time step (i-1), m/s.
$Y (i-1)$ = position component in z direction at time step (i-1), m/s.

Equations (6) through (12) were used to develop a computer model to predict the droplet size diameter distribution. The input data were nozzle shape, nozzle dimensions, Trajectory angle, riser height, orifice coefficient, wind speed and direction. The flowchart of the model is illustrated in Fig. (1).

The initial conditions (at zero time) required to run the model, are as follows:

$X(0)$ = 0
$Z(0)$ = riser height (1 m in this study)
$V(0)$ = nozzle water velocity, m/s
θ_0 = nozzle trajectory angle, deg
$V_x (0) = V(0) \cos \theta_0$, $V_y (0) = V(0) \sin \theta_0$

A 0.1 mm droplet diameter increment was used starting from 0.1 mm to maximum droplet diameter. Finally the model gives the droplet diameter and its distance from sprinkler as an output.

DATA GENERATION FOR THE MODEL:

190

To generate the data required for the model, indoors lab test runs were conducted. The sprinkler system used an electric pump of 0.37 kW with ¾ inch inlet diameter and ¾ inch outlet diameter. The pipeline used was polyethylene pipe of ¾ inch nominal diameter. The riser height was 100 cm. Riser was steel pipe of ¾ inch nominal diameter. The R.C. 160-S sprinkler was used in this study. The sprinkler material was plastic, full circle ¾ inches male pipe thread connection. The nozzle dimensions were square (3.9 mm), rectangle (3 mm width x 5 mm height), isosceles triangle (5.5 mm - base and height) and circle (4.4 mm diameter) with trajectory angle 20°. The cross section areas of the four shapes are almost the same except of the very small fractions due to mathematical transformation from one shape to another. Moreover, the possibility of manufacturing these different shapes at the exact cross section areas. The *Petri* dishes used were 89 mm in diameter and 16 mm in height. Misr 10000 Km oil was used in this study.

The droplet photographic instrument adopted illumination technique was used to measure the droplet size diameter. Nicon coolpix 5600 Digital Camera was used in the study to photo the *Petri* dishes with oil using close- up mode. It was 5.1 mega pixels and 3X zoom. The Image-Pro Plus for windows version 1.3 program was used in this study to measure the droplet diameter from the photos of *Petri* dishes with oil and water droplets.

Four levels of pressure were used: 138, 172.5, 207 and 240 kPa (20, 25, 30 and 35 Psi). Four shapes of nozzles were tested: square, rectangle, triangle and circle. Testes were replicated 3 times. So, the total number of experiments was 48. Pressure was measured using the dial pressure gage 60 Psi (414 kPa) with scale increment of 2 Psi (13.8 kPa). The location of the pressure gage was fixed at 92.5 cm from the lateral as recommended by the *ASABE standard (2006)*.

The duration of each replicate was one path only of the sprinkler. The water droplets were collected in *Petri* dishes filled with oil. To ensure credibility, the actual droplet diameter (Calculated by volume mean weight diameter procedure) was correlated to the measured ones (collected in the *Petri* dishes). The latter was determined via a digital

camera and the Image Pro software. The following correlation was obtained

$$\text{ADSD} = 0.99 \text{ MDSD} + 0.0244 \qquad\qquad (13)$$

Where:

ADSD = Actual droplet size diameter, mm

MDSD = Measured droplet size diameter, mm

Based on these results, very small difference was neglected and the actual droplet size diameter was assumed the same as the measured droplet diameter.

This model may be used only for zero wind condition. However, it was modified to be used in windy condition.
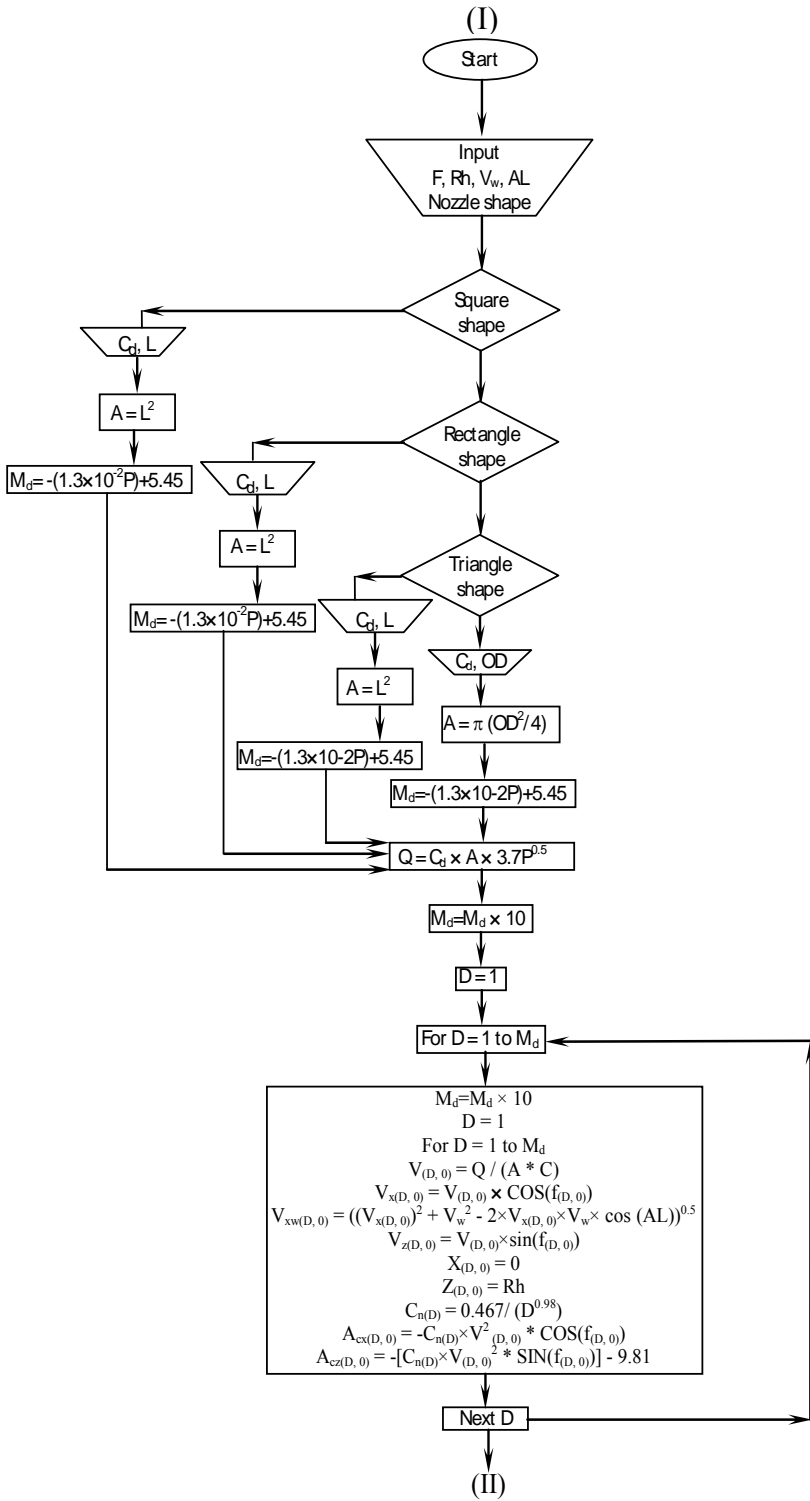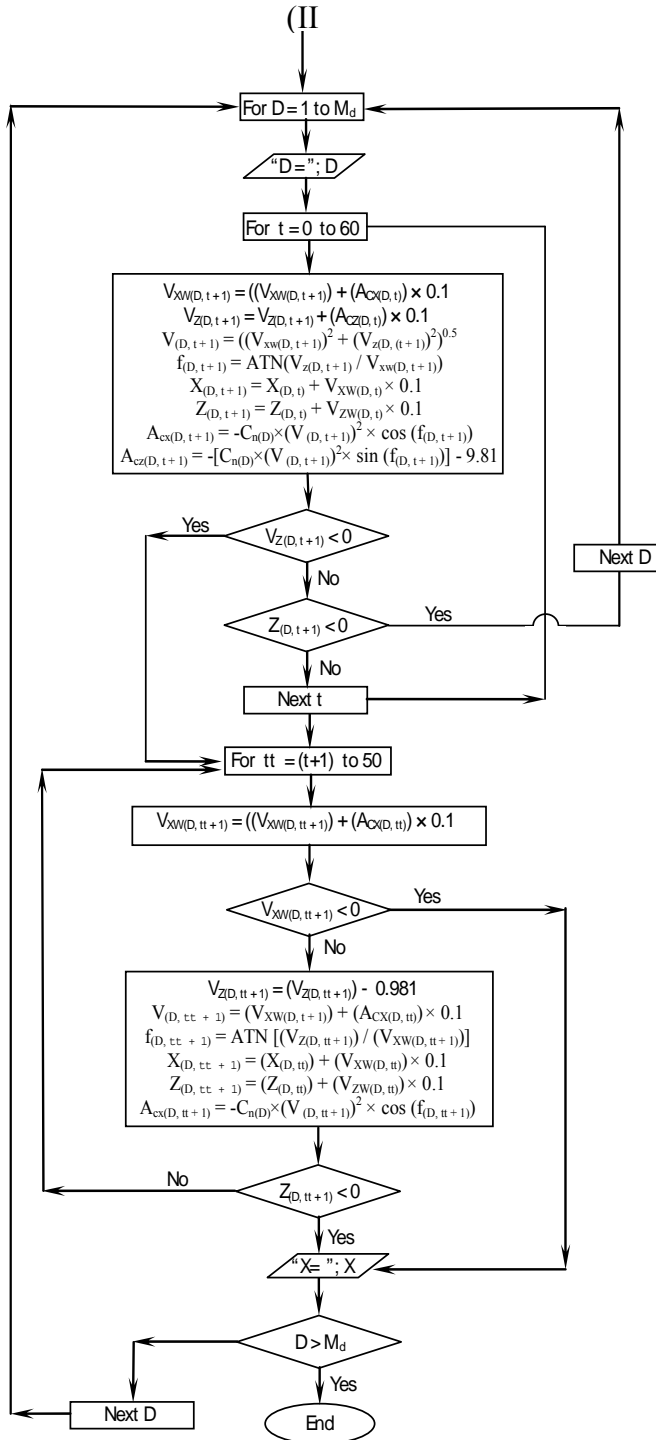
(I)

Start

Input
F, Rh, V_w, AL
Nozzle shape

Square shape

C_d, L

$A = L^2$

$M_d = -(1.3 \times 10^{-2} P) + 5.45$

Rectangle shape

C_d, L

$A = L^2$

$M_d = -(1.3 \times 10^{-2} P) + 5.45$

Triangle shape

C_d, L

$A = L^2$

$M_d = -(1.3 \times 10 - 2P) + 5.45$

C_d, OD

$A = \pi (OD^2/4)$

$M_d = -(1.3 \times 10 - 2P) + 5.45$

$Q = C_d \times A \times 3.7 P^{0.5}$

$M_d = M_d \times 10$

$D = 1$

For $D = 1$ to M_d

$M_d = M_d \times 10$
$D = 1$
For $D = 1$ to M_d
$V_{(D, 0)} = Q / (A * C)$
$V_{x(D, 0)} = V_{(D, 0)} \times COS(f_{(D, 0)})$
$V_{xw(D, 0)} = ((V_{x(D, 0)})^2 + V_w^2 - 2 \times V_{x(D, 0)} \times V_w \times \cos (AL))^{0.5}$
$V_{z(D, 0)} = V_{(D, 0)} \times \sin(f_{(D, 0)})$
$X_{(D, 0)} = 0$
$Z_{(D, 0)} = Rh$
$C_{n(D)} = 0.467/ (D^{0.98})$
$A_{cx(D, 0)} = -C_{n(D)} \times V^2_{(D, 0)} * COS(f_{(D, 0)})$
$A_{cz(D, 0)} = -[C_{n(D)} \times V_{(D, 0)}^2 * SIN(f_{(D, 0)})] - 9.81$

Next D

(II)

Figure (1): Flowchart of the developed computer model.

193

(II

For D = 1 to M_d

"D = "; D

For t = 0 to 60

$V_{XW(D, t+1)} = ((V_{XW(D, t+1)}) + (A_{CX(D, t)}) \times 0.1$
$V_{Z(D, t+1)} = V_{Z(D, t+1)} + (A_{CZ(D, t)}) \times 0.1$
$V_{(D, t+1)} = ((V_{xw(D, t+1)})^2 + (V_{z(D, (t+1)}))^2)^{0.5}$
$f_{(D, t+1)} = ATN(V_{z(D, t+1)} / V_{xw(D, t+1)})$
$X_{(D, t+1)} = X_{(D, t)} + V_{XW(D, t)} \times 0.1$
$Z_{(D, t+1)} = Z_{(D, t)} + V_{ZW(D, t)} \times 0.1$
$A_{cx(D, t+1)} = -C_{n(D)} \times (V_{(D, t+1)})^2 \times \cos(f_{(D, t+1)})$
$A_{cz(D, t+1)} = -[C_{n(D)} \times (V_{(D, t+1)})^2 \times \sin(f_{(D, t+1)})] - 9.81$

Yes ← $V_{Z(D, t+1)} < 0$

No

$Z_{(D, t+1)} < 0$ → Yes

No

Next t

Next D

For tt = (t+1) to 50

$V_{XW(D, tt+1)} = ((V_{XW(D, tt+1)}) + (A_{CX(D, tt)}) \times 0.1$

$V_{XW(D, tt+1)} < 0$ → Yes

No

$V_{Z(D, tt+1)} = (V_{Z(D, tt+1)}) - 0.981$
$V_{(D, tt+1)} = (V_{XW(D, tt+1)}) + (A_{CX(D, tt)}) \times 0.1$
$f_{(D, tt+1)} = ATN[(V_{Z(D, tt+1)}) / (V_{XW(D, tt+1)})]$
$X_{(D, tt+1)} = (X_{(D, tt)}) + (V_{XW(D, tt)}) \times 0.1$
$Z_{(D, tt+1)} = (Z_{(D, tt)}) + (V_{ZW(D, tt)}) \times 0.1$
$A_{cx(D, tt+1)} = -C_{n(D)} \times (V_{(D, tt+1)})^2 \times \cos(f_{(D, tt+1)})$

No ← $Z_{(D, tt+1)} < 0$

Yes

"X= "; X

$D > M_d$

Yes

End

Next D

Cont. Figure (1): Flowchart of the developed computer model.

194

SIMULATING WIND EFFECT:

During the sprinkler rotation the angle between wind direction and droplet movement direction (α) changed from 0° to 360°. When $\alpha = 0°$ the resultant velocity (V_{xw}) is the summation of water droplet velocity and wind velocity as shown in Figure (2). But when $\alpha = 180°$ as shown in Figure (3) the resultant velocity (V_{xw}) is the difference between water droplet velocity and wind velocity. In general case when $0° < \alpha < 360°$ as shown in Figure (4) V_{xw} could be described by the following equation:
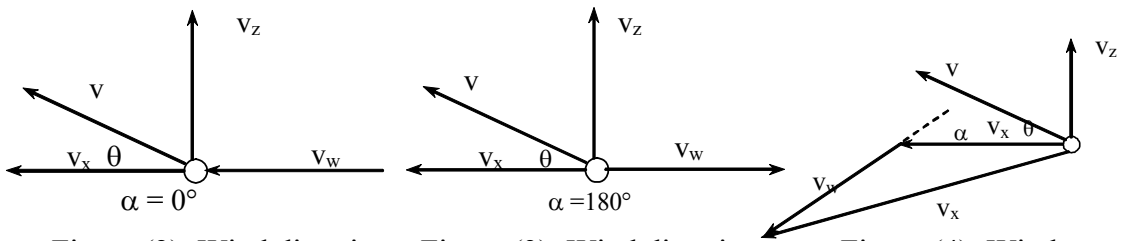
Figure (2): Wind direction with the same direction as droplet (α = zero°).

Figure (3): Wind direction with the opposite direction of droplet (α = 180°).

Figure (4): Wind direction with α angle direction of droplet.

$$V_{xw} = \sqrt{v_x^2 + v_w^2 - 2v_x v_w \cos (180 - \alpha)} \qquad (14)$$

Where:

v_x = Droplet velocity component in x direction (m.s^{-1})

v_w = Wind velocity (m.s^{-1})

v_{xw} = Droplet resultant velocity in x direction for windy condition (m.s^{-1})

v_x = v Cos θ

α = angle between wind direction and droplet movement direction (deg.)

MODEL VERIFICATION:

To verify the model output, the predicated values were correlated to the measured values. A linear regression model of Y=A+BX was developed with the predicted droplet diameter as the dependent variable (Y) and the observed droplet diameter as the independent variable (X). If the regression model was a perfect predictor of the droplet diameter, the

195

linear regression constants (A) and (B) would equal 0 and 1, respectively. **_Gregory and Fedler (1986)_** stated that values or R^2 (coefficient of determination) varies between 0 and 1 and provides an index of goodness of model fit. If R^2 value is 0.90 or larger, then at least 90% of the variability is explained. This would generally be considered an excellent fit. On the other hand, an R^2 value of 0.80 is considered a good fit. An R^2 value as low as 0.60 is sometimes considered acceptable or even good. The evaluation of linear model of different shapes is based on values of A, B, R^2, R and the standard error of estimation (λ) which is defined below as:

$$\lambda = \sqrt{\frac{\sum_{i=1}^{i=n}\left(D_{Mes.} - D_{Pre.}\right)^2}{n}} \qquad (15)$$

Where:

$\quad D_{Mes}$ = Measured droplet diameter, mm.
$\quad D_{Pre.}$ = Predicted droplet diameter, mm.
$\quad \lambda$ = Standard error of estimation
$\quad n$ = Number of observations.

The R^2 and λ (standard error of estimate linear model) indicate the scatter points about the regression equation. R (correlation coefficient) indicates the degree of association between the observed and predicted values. To assist further in this evaluation, another index called coefficient of efficient (C_e) was used. This coefficient was proposed by **_Nash and Sutcliffe (1970)_** and used by **_Masheshwari and McMahon (1993)_**, **_Zin El-Abedin and Ismail (1999)_** and **_Sharaf (2003)_**. If R and C_e are close to each other, the model is free from any bias all or part of the data. C_e is defined below as:

$$C_e = \frac{\sum_{i=1}^{i=n}\left(X_{oi} - \overline{X}_o\right)^2 - \sum_{i=1}^{i=n}\left(X_{oi} - X_{pi}\right)}{\sum_{i=1}^{i=n}\left(X_{oi} - \overline{X}_o\right)^2} \qquad (16)$$

Where:

$\quad C_e$ = coefficient of efficient
$\quad n$ = number of observations
$\quad X_{oi}$ = i^{th} value of observed measurements, mm.
$\quad \overline{X}_o$ = average observed value, mm.
$\quad X_{pi}$ = i^{th} value of predicted measurements, mm.

196

The arithmetic mean droplet size distribution from data generation experiment results for different nozzle orifice shapes and sprinkler base pressures are shown in following Table.

Table (1): Arithmetic mean droplet size diameter (mm) for different nozzle   orifice shapes and sprinkler base pressures along the throw.

Sprinkler base pressure, kPa	Nozzle orifice shape	Distance from sprinkler, m						
		1	3	5	7	9	11	13
137.0	Circular	0.37	0.78	1.31	1.5	2.8	3.76	
	Square	0.78	0.98	1.38	2.58	3.08		
	Rectangular	0.65	0.97	1.53	2.39			
	Triangular	0.51	0.91	1.51	2.47			
172.5	Circular	0.31	0.77	1.28	1.32	2.39	3.04	
	Square	0.48	0.85	1.31	1.97	2.83		
	Rectangular	0.47	0.89	1.33	2.08	2.27		
	Triangular	0.51	0.83	1.36	1.98	2.4		
207.0	Circular	0.3	0.73	0.94	1.11	1.55	2.4	2.83
	Square	0.43	0.77	1.27	1.71	2.62		
	Rectangular	0.44	0.77	1.26	1.57	2.21		
	Triangular	0.5	0.8	1.35	1.68	2.31		
241.5	Circular	0.26	0.69	0.86	0.99	1.29	2.04	2.34
	Square	0.41	0.77	1.08	1.5	2.12		
	Rectangular	0.38	0.77	1.05	1.26	2.08		
	Triangular	0.48	0.8	1.05	1.61	2.2		

MAXIMUM DROPLET SIZE DIAMETER:

The model requires the maximum droplet size diameter for each orifice shape and sprinkler base pressure. Using previous indoor lab testes results in the following linear equations developed to describe the relationship between maximum droplet size diameter and sprinkler base pressure for circular, square, rectangular and triangular orifice shapes respectively.

For circle   : MD = -0.0130 Pr + 5.45 $R^2 = 0.96$ (17)
For square   : MD = -0.0089 Pr + 4.36 $R^2 = 0.96$ (18)
For rectangle   : MD = -0.0028 Pr + 2.77 $R^2 = 0.99$ (19)
For triangle   : MD = -0.0025 Pr + 2.81 $R^2 = 0.99$ (20)

Where:
        MD = Maximum droplet size diameter, mm
        Pr   = Sprinkler base pressure, kPa

1- For different orifice shapes:

A graphical comparison of the measured versus predicted droplet size diameter for different shapes; circle, square, rectangle and triangle are given in Figure (5).

In general, the value of B is close to 1 and A close to zero, accompanied by low λ and high R^2, R and C_e values, would indicate satisfactory prediction by the model. Because the slope B and the intercept A are significantly different from 1.0 and 0, respectively, at the 99% level of confidence, a bias exists within the model estimation. This bias oscillates between over and less estimation which depends mainly on A and B values. The results of this evaluation along with the statistical parameters for droplet diameters are given in Tab. (2)

Table (2): Indices of the different orifice shapes
in predicting droplet diameter.

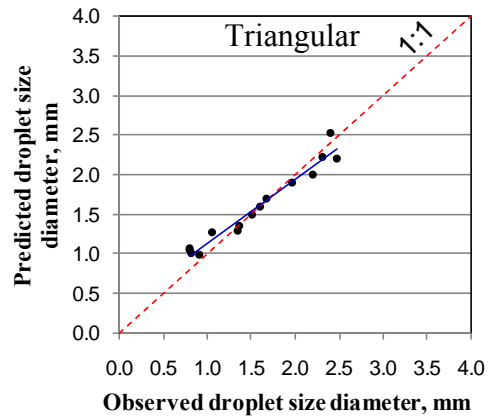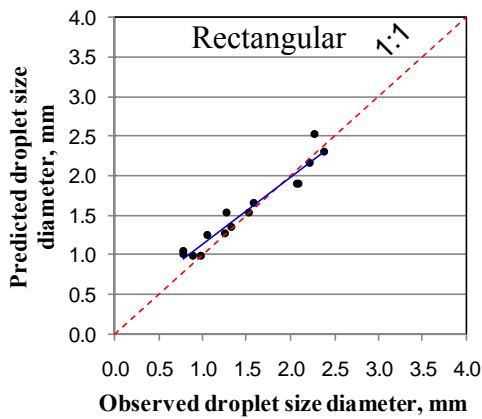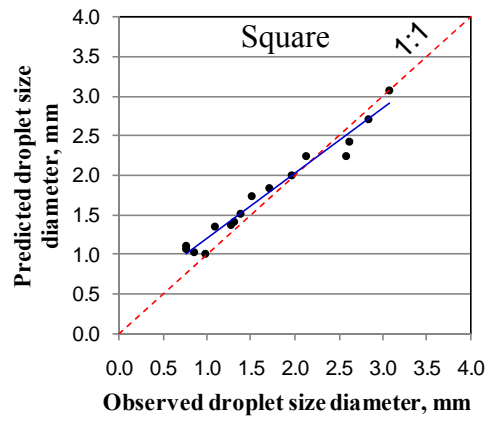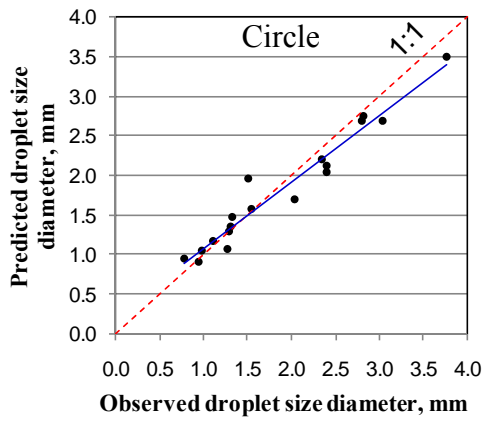| Parameter	Circle	Square	Rectangle	Triangle
n	18	16	15	15
A	0.842	0.818	0.839	0.802
B	0.233	0.382	0.311	0.334
C_e	0.912	1.142	1.232	1.083
R^2	0.949	0.968	0.935	0.957
R	0.974	0.984	0.967	0.978
λ	0.217	0.191	0.168	0.155

198

Figure (5): Verification of droplet size diameter
for different orifice shapes.

Considering the value of various indices of evaluating the four shapes, one can find that R^2 values for all shapes are greater than 0.93 and C_e values are close to R^2. The value of A and B are closer to 1 and 0 respectively. Furthermore, R^2 values are high, less difference between R^2 and C_e and λ values are minimal.

In general, the correlation between the observed and predicted droplet diameter values for all shapes is satisfactory. This indicates that the model output is appropriate and the bias existing within the shapes can be attributed to the experimental errors, manufacturer variation and uncalculated factors.

2- For different sprinkler base pressures:

A graphical comparison of the measured versus predicted droplet diameters for different sprinkler base pressures 138 kPa, 172.5 kPa, 207 kPa and 241.5 kPa are given in Figure (6).

In general, the value of B was close to 1 and A close to zero, accompanied by low λ and high R^2, R and C_e values, would indicate satisfactory prediction by the model. Because the slope B and the intercept A are not significantly different from 1.0 and 0, respectively, at the 99% level of confidence, a bias exists within the model estimation. This bias oscillates between over and less estimation which depends mainly on A and B values. The results of this evaluation along with the statistical parameters for droplet diameters are given in Tab. (3)

Considering the value of various indices of evaluating the four shapes, one can find that R^2 values for all sprinkler base pressures are greater than 0.91 and C_e values are close to R^2. The value of A and B are close to 1 and 0 respectively. Moreover, R^2 values are high, less difference between R^2 and C_e and λ values are minimal.

Table (3): Indices of the different sprinkler base pressures
in predicting droplet diameter.

Parameter	138 kPa	172.5 kPa	207 kPa	241.5 kPa
n	15	16	17	16
A	0.863	0.852	0.817	0.597
B	0.246	0.251	0.322	0.519
C_e	0.990	0.985	1.073	1.296
R^2	0.964	0.937	0.971	0.913
R	0.982	0.968	0.985	0.956
λ	0.189	0.181	0.151	0.218

In general, the correlation between the observed and predicted droplet diameter values for low sprinkler base pressures 138 kPa, 172.5 kPa and 207 kPa are more satisfactory than the high pressure of 241.5 kPa.
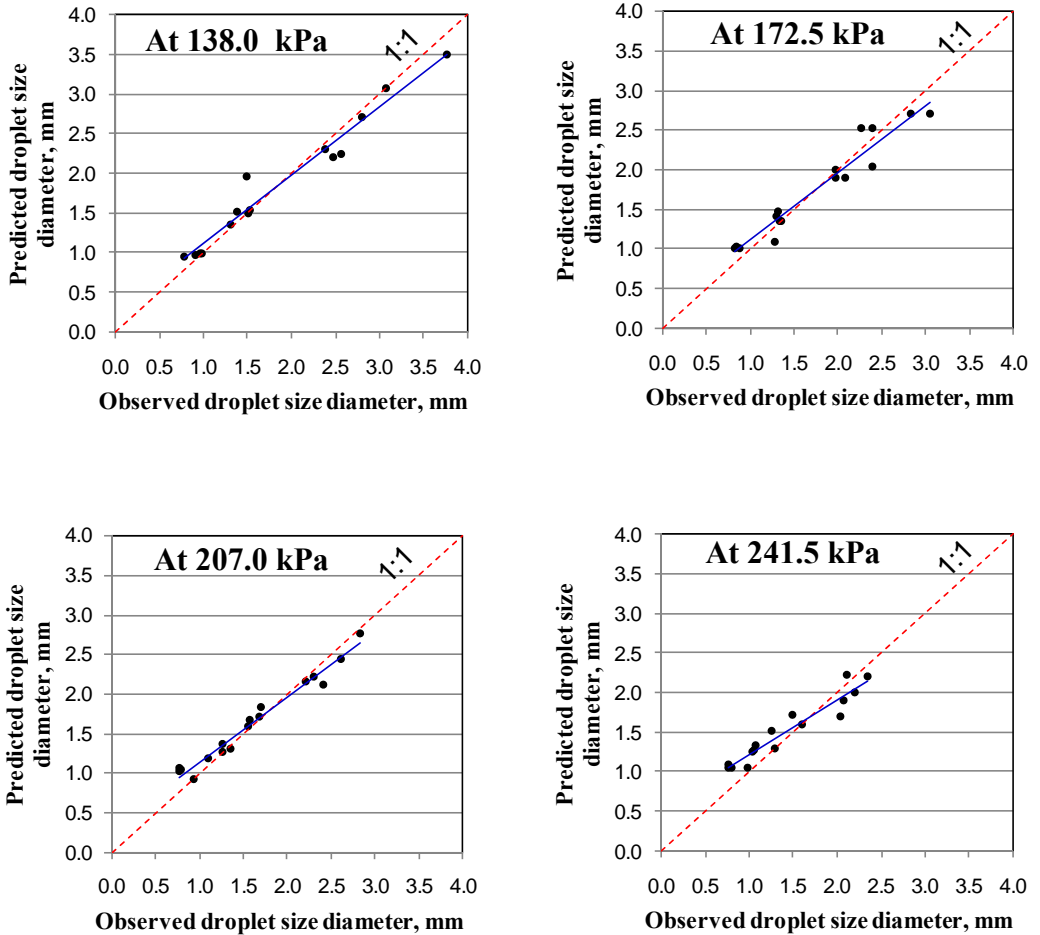

Figure (6): Verification of droplet size diameter for different Sprinkler base pressures.

CASE STUDY

The objectives of this case study were to:

1-   Compare the droplet size distribution model prediction in zero and windy conditions.

2-   Predict the wetted pattern shape in zero and windy conditions.

The computer model was used to simulate the effect of wind speed on droplet size distribution in windy conditions (up and down wind). Wind elongated the pattern at right angles to the wind (i.e. crosswind). The wetted distance downwind from the sprinkler (B) increased as wind velocity increased but the increase was proportionally less than the decrease in wetted distance upwind (A) (Table 4 and Figures 7 and 8). As a result, increasing wind velocity decreased the wetted area. The previous results agree with those obtained by *Richards and Weatherhead (1993).* Figure (7) is showing the difference between droplet size distribution at zero and windy conditions (i.e. 1, 2, 3 and 4 m/s) for the triangular orifice nozzle shape.

The model also can predict the droplet size distribution at any wind direction overall the irrigated pattern. Also the model can predict the shape of the wetted pattern at zero and windy conditions. The model was run at different wind speeds and 0° to 360° wind direction with interval of 10° to get the maximum throw. The angle (wind direction) and maximum throw were used to draw the pattern shape using the Autocad software. Figure (8) illustrates the wetted perimeter from zero to 10 m/s wind speed.

Table (4): distance up and down wind from the sprinkler
with different wind speeds.

Wind speed, m/s	distance upwind, mm (A)	distance downwind, mm (B)
1	0.46	0.44
2	0.96	0.86
3	1.49	1.25
4	2.07	1.62
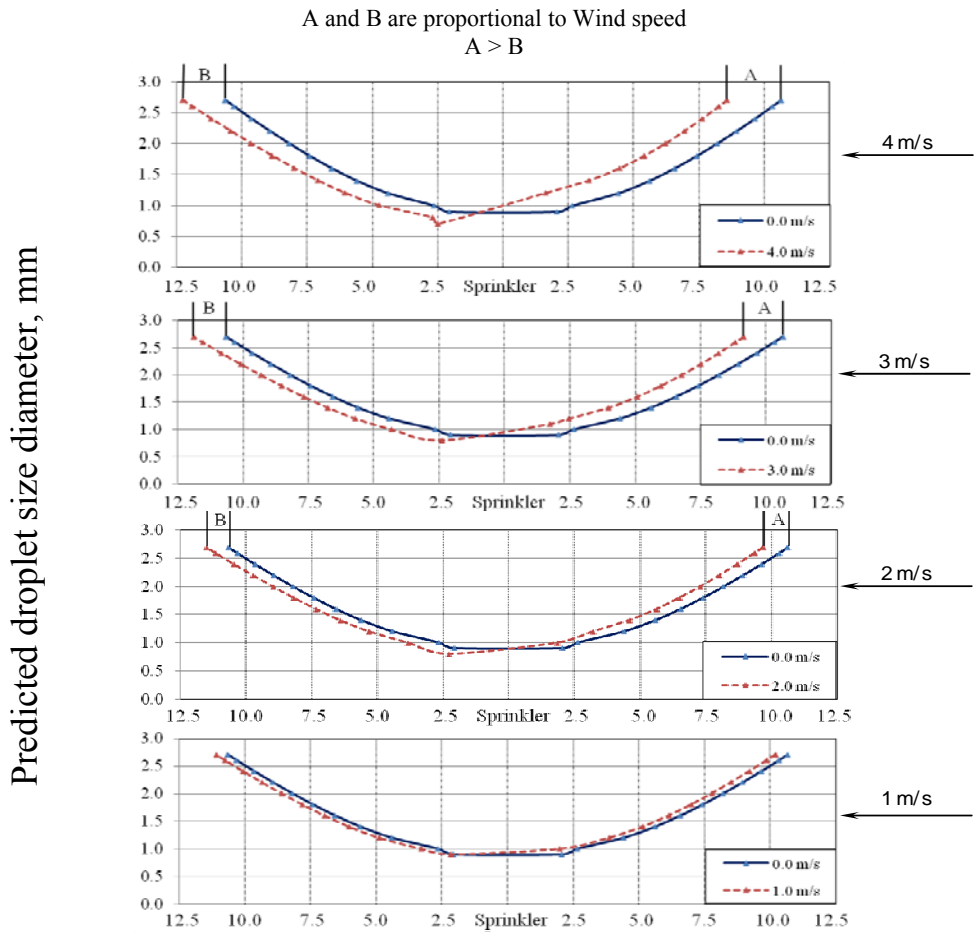
Figure (7): Effect of wind speed on droplet size distribution
compared with zero wind condition.

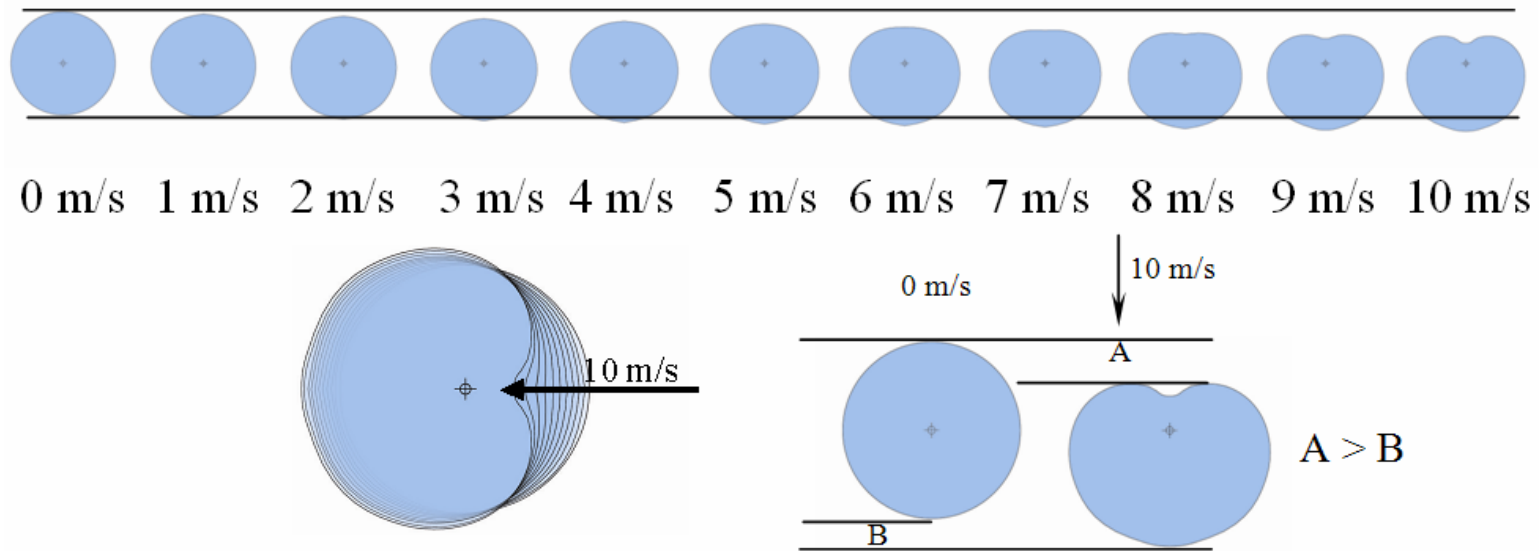0 m/s 1 m/s 2 m/s 3 m/s 4 m/s 5 m/s 6 m/s 7 m/s 8 m/s 9 m/s 10 m/s

Figure (8): Effect of wind speed on application pattern from zero to 10 m/s wind speed and intervals of 1 m/s.

CONCLUSIONS

A computer model was developed to predict the droplet size distribution with zero and windy conditions. The model was Verified for different orifice shapes (circle, square, rectangular and triangle) and different pressures (138.0, 172.5, 207.0 and 241.5 kPa). The best results of the computer model predictions were achieved with triangular and rectangular nozzles; then with square and finally circular nozzle. For working pressures; the best results were attained at 207.0 and 172.5 kPa then 138.0 kPa and finally 241.5 kPa. In general, the correlation between the observed and predicted droplet size diameter values for all sprinkler base pressures and shapes is quite good. The model was used to predict the pattern shape in no wind and windy conditions. Wind elongated the pattern at right angles to the wind. The wetted distance downwind from the sprinkler increased as wind velocity increased but the increase was proportionally less than the decrease in wetted distance upwind. As a result, increasing wind velocity decreased the wetted area.

REFERANCES

ASABE Standards 2006. Standards Engineering Practices Data. Procedure for sprinkler testing and performance reporting. S398.1. PP 933-935.Adopted and published by the American Society of Agricultural and Biological Engineers. 53rd. Edition. ASABE, St.Joseph, MI, USA.

Awady, M. N. 1978. An atomization theory for swirl nozzles, *Trans. of the ASAE 21* (1): 70-74.

Chen, D.and W. W. Wallender. 1985. Droplet size distribution and water application with low-pressure sprinklers. *Trans. of the ASAE* 28 (2): 511-516.

Hills, D.J. and Yuping Gu, 1989. Sprinkler volume mean droplet diameter as a function of pressure. *Trans. of the ASAE* 32 (2): 471-476.

Forst, K.R. and H.C. Schwalen 1960. Evapotranspiration sprinkler irrigation. *Trans. of the ASAE* 3 (1): 18-20.24.

Gregory,J.M. and C.B. Fedler, 1986. Model evaluation and research verification (MERV). ASAE Paper No. 86-5032.

Heernann, D.F. and R.A. Kohl, 1981. Fluid dynamics of sprinkler systems. P: 583-618 Cited from Design and operation of farm irrigation systems. 859

P. Ed. M. E. Jensen. An ASAE Monograph, No.3, ASAE, 2950 Niles Rd. St. Joseph MI, USA.

James L.G. and Blair S.K. 1984. Performance of low pressure center pivot systems. *Trans. of the ASAE* 27(6):1753-1757.

Jiusheng Li and Hiroshi Kawano, 1995. Simulating water-droplet movement from noncircular sprinkler nozzles. *J. Irrig. Drain. Div. ASCE* 121 (2): 152-185.

Jiusheng Li, 1997. Effect of pressure and nozzle shape on the characteristics of sprinkler droplet spectra. J. Agric. Eng. Research, Vol. 66, no. 1: 15-21.

Kohl, R. A. 1974 . Droplet size distribution from medium-size agricultural sprinklers. *Trans. of the ASAE* 17 (4): 690-693.

Larry G. james 1988. Principles of farm irrigation system design. 541: P. 192,197.

Maheshwari, B. L. and T. A. Mcmahon, 1993. Performance evaluation of border irrigation models for south-east Australia: Part I, Advance and Recession characteristics. J. of Ag. Eng. Res. 54: 67-87.

Nash, J.E. and J.V. Sutcliffe, 1970. River flow forecasting through conceptual models. I.A. discussion of principles. J. of Hydrology, 10: 282-324.

Richards, P. J. and E.K. Weatherhead. 1993. Prediction of rain gun application patterns in windy conditions. J. Agric. Eng. Research 54(4): 281-291

Seginer, I. 1965. Tangential velocity of sprinkler drops. *Trans. of the ASAE* 3 (1): 90-93.

Seginer, I. 1971. Water losses during sprinkling. *Trans. of the ASAE* 14 (4): 656- 659, 664.

Sharaf, G.A. 2003. Evaluation of pressure distribution and lateral flow rates along drip tape lateral. J. Agric. Eng., Research 20(2): 542-556.

Zin El-Abedin, T. K. and S. M. Ismail, 1999. Estimation and analysis of water advance in surface irrigation. Misr J. Ag. Eng., 16 (4): 720-744.

الملخص العربي

برنامج بالحاسب الالكتروني للتنبؤ بمسافة سقوط قطرات المياه في ظروف انعدام الرياح وعند سرعات رياح مختلفة لأشكال مختلفة من فوهات الري بالرش

عزمي البري[1]، محمود هانئ رمضان[2]، محسن عبد السلام العدل[3]، هاشم محمد عبدالمجيد[4]

نظراً لتأثير حجم القطرات الكبير على سطح التربة. وزيادة نسبة الفاقد بالبخر والرياح للقطرات الصغيرة تم دراسة توزيع القطرات لأشكال مختلفة من فوهات الرشاشات (المربع والمستطيل والمثلث والدائرة). تم عمل برنامج بالحاسب الالكتروني للتنبؤ بتوزيع أحجام قطرات الرش للرشاشات ذات أشكال الفوهات المربعة والمستطيلة والمثلثة ومقارنتها بالفتحة الدائرية في كلٍ من ظروف عدم وجود رياح وكذلك في ظروف تواجد رياح بسرعات مختلفة. بناءً على ذلك أجريت مجموعة من التجارب المعملية لقياس قطر قطرات الرش على طول مسار مرمى الرش عند ضغوط تشغيل 138، 172,5، 207، 241,5 كيلوبسكال للأشكال المختلفة قيد الدراسة. أوضحت النتائج أن الضغط يتناسب تناسبا عكسيا مع حجم القطرات وأن شكل فتحة الرشاش تؤثر على توزيع القطرات. بتطبيق البرنامج مع نفس الأشكال والضغوط ومقارنة النتائج المحسوبة من مخرجات البرنامج مع النتائج المعملية تبين أن القيم التي يتنبأ بها البرنامج متوافقة مع القيم المقاسة معملياً بمعامل ارتباط أكبر من 0,9 وذلك للشكل المثلث والمستطيل والمربع والدائرة على التوالي. ومن حيث الضغوط كان أكبر ارتباط لنتائج ضغوط 207، 172,5 ثم 138 كيلوبسكال ويليه 241,5 كيلو بسكال. بشكل عام تبين ملائمة البرنامج للتنبؤ بتوزيع القطرات لجميع الأشكال والضغوط بشكل جيد. في ظروف وجود الرياح ، أوضحت نتائج البرنامج نقص قطر الابتلال في اتجاه هبوب الرياح وزيادته في الجهة المقابلة. كما أوضحت أن النقص في اتجاه هبوب الرياح أكبر من الزيادة في الاتجاه المقابل ، مما يترتب عليه أن المساحة المبتلة تتناسب تناسباً عكسياً مع سرعات الرياح. كما أن البرنامج يمكنه التنبؤ بشكل دائرة الابتلال في ظروف سرعات الرياح المختلفة لجميع الأشكال والضغوط. أدخلت نتائج البرنامج على برنامج الأوتوكاد لرسم شكل دائرة الابتلال للرشاش ذي الفوهة المثلثة (كحالة دراسة) تحت ظروف سرعات رياح مختلفة.

1 أستاذ الهندسة الزراعية ـ كلية الزراعة ـ جامعة القاهرة.2و3 أستاذ مساعد الهندسة الزراعية ـ كلية الزراعةـ جامعة المنصورة. 4 باحث مساعد محطة بحوث واختبار الجرارات ـ معهد بحوث الهندسة الزراعية – وزارة الزراعة